NASA
Technical Memorandum 86430

AVSCOM
Technical Report 85-B-5

Effect of Measured Material Properties on the Finite Element Analysis of an OH-58 Composite Tail Boom

Lynn M. Bowman

OCTOBER 1985

NASA

U.S. ARMY AVIATION SYSTEMS COMMAND

NASA
Technical Memorandum 86430

AVSCOM
Technical Report 85-B-5

Effect of Measured Material Properties on the Finite Element Analysis of an OH-58 Composite Tail Boom

Lynn M. Bowman
Aerostructures Directorate
USAARTA-AVSCOM
Langley Research Center
Hampton, Virginia

National Aeronautics
and Space Administration

**Scientific and Technical
Information Branch**

1985

SUMMARY

A static and dynamic finite element analysis was conducted on a U.S. Army OH-58 composite tail boom and compared with test data. The tail boom was a filament-wound graphite/epoxy monocoque structure. The structural design of the composite tail boom skin was based on 50-percent graphite fiber volume. However, material tests on representative samples of the tail boom skin revealed that the graphite fiber-volume fraction varied from 44.6 to 49.3 percent. To determine the effect of using measured material properties, static and dynamic finite element analyses were conducted for three fiber-volume conditions of 45, 48, and 50 percent. The static and dynamic model with the 45-percent fiber-volume graphite skins gave the closest agreement with test data.

INTRODUCTION

For years, the U.S. Army has been committed to applying advanced composite technology to helicopter components and airframe structures. During the period from March 1978 to February 1982, 11 composite tail booms were fabricated and then installed on U.S. Army OH-58 light observation-type helicopters for evaluation purposes (ref. 1). A prototype tail boom was made available for in-house structural testing and evaluation, and a comparison was made with a finite element model of the composite tail boom.

The purpose of this paper is to present the results of a static and dynamic finite element analysis of the OH-58 composite tail boom. The tail boom design, which is a wet-filament-wound graphite/epoxy monocoque, and a material property determination are discussed. A description of the finite element models is presented. Results of the finite element analysis, which consist of static displacements and fundamental natural frequencies, are compared with the experimental data from reference 2.

SYMBOLS

E_f fiber elastic modulus, lb/in^2

E_m matrix elastic modulus, lb/in^2

E_{11} longitudinal elastic modulus, lb/in^2

E_{22} transverse elastic modulus, lb/in^2

G_f fiber shear elastic modulus, lb/in^2

G_m matrix shear elastic modulus, lb/in^2

G_{12} composite shear elastic modulus, lb/in^2

v_f fiber-volume fraction

v_m matrix-volume fraction

W_c composite weight, lb

W_f fiber weight, lb

X,Y,Z translational directions (see fig. 6)

ν_f fiber Poisson's ratio

ν_m matrix Poisson's ratio

ν_{12} longitudinal Poisson's ratio

ρ_c composite density, lbm/in^3

ρ_f fiber density, lbm/in^3

DESCRIPTION OF OH-58 COMPOSITE TAIL BOOM

Figure 1 shows a typical Army OH-58 helicopter. The OH-58 composite tail boom was a monocoque structure composed of graphite/epoxy ring frames and filament-wound unstiffened skin. Figure 2 shows the tail boom stations, the skin ply-stacking sequence, and the ply orientation used for the skins. The tail boom, which begins at station 32 and ends at station 183, is 151 in. long. The station numbers are distances in inches measured from a referenced location on the fuselage.

Figure 3 shows a plan view and side view of the tail boom with cross-sectional views of individual components. The ring frames, as depicted in figure 3, were made of woven graphite/epoxy fabric overwrapping a urethane foam core. The ring frames were precured and then incorporated in a collapsible mandrel. Next, the skins were wound on the mandrel by using wet-filament-wound Thornel[1] 300 graphite (3000 filament tow) with Applied Plastics Corporation (APCO) 2434/2345 epoxy resin.

The forward-attachment ring was a hand lay-up and was made of 25 plies of E-glass fabric. The forward-attachment fitting was made of wet-filament-wound S-glass overwrapped on a 6061-T6 aluminum-alloy insert. The aluminum insert is depicted by hatched lines in cross-sectional view A-A of figure 3. Exterior support components, such as the stabilizer mounts and end vertical-fin supports, were made of E-glass fabric and secondarily bonded to the tail boom. Reference 1 contains a detailed description of the entire fabrication process.

MATERIAL PROPERTY DETERMINATION

Mechanical properties of filament-wound structures can be affected by design and manufacturing variables. These variables are winding pattern, filament tension, cure cycle, resin content, fiber orientation, skin thickness, void content, and others (ref. 3). Because the tail boom was filament wound, a material property investigation on a second representative tail boom was conducted in order to determine which elastic properties to use for the graphite/epoxy skins. The second tail boom was cut

---

[1]Thornel: Registered trademark of the Union Carbide Corporation.

into nine cross-section parts. Skin thickness measurements were conducted on all the cross sections, and one of these sections (station 49) was tested to determine the graphite fiber-volume fraction.

Large variations in skin thickness were identified circumferentially and longitudinally along the tail boom. Figure 4 shows the skin thicknesses measured at station 49. The minimum and maximum measured thicknesses of all the cross sections and the design thickness at each station are presented in table I. All the measured skin thicknesses include the paint thickness. Photomicrographs were taken of two sections at station 49 to determine the typical void content of the skin. As shown in figure 5, the voids were visible and randomly scattered throughout the ring. Using the photomicrographs in figure 5, the void content was determined from the ratio of the total void area to the total area. Typical void contents of 1.5 and 5.0 percent were calculated. Photomicrographs were also used to determine the thickness of the paint, which was found to be between 0.001 and 0.002 in.

In order to determine the graphite/epoxy fiber volume, material tests were conducted to obtain typical densities and graphite fiber weights from three sections (6, 14, and 20) on station 49. The density of each graphite/epoxy specimen was determined by a liquid displacement method described in reference 4. The fiber weight of each specimen was determined by using an acid digestion technique in accordance with procedures described in reference 5. Using the results for the densities and fiber weights obtained from the material tests, the fiber-volume fraction v_f was determined for each graphite/epoxy specimen by using

$$v_f = \frac{W_f/\rho_f}{W_c/\rho_c} \tag{1}$$

where W_f, W_c, ρ_f, and ρ_c are fiber weight, composite weight, fiber density, and composite density, respectively. (See ref. 6.) The composite density and fiber-volume fraction for each specimen are listed in table II. Variations in density and fiber-volume fraction were present (44.6 to 49.3 percent). The sensitivity of density to the presence of voids for these specimens was less than 1 percent and thus negligible. Therefore, the densities used in this study do not account for the presence of voids.

Based on table II, inplane mechanical properties of the graphite/epoxy skin were calculated for fiber-volume fractions of 45 and 48 percent. These properties and the design inplane mechanical properties, which were based on a fiber-volume fraction of 50 percent, are used in the finite element analysis of the tail boom.

The longitudinal elastic modulus E_{11} and Poisson's ratio ν_{12}, given as

$$E_{11} = v_f E_f + v_m E_m \tag{2}$$

$$\nu_{12} = v_f \nu_f + v_m \nu_m \tag{3}$$

were obtained by the "rule of mixtures" (refs. 7, 8, and 9) where v_f, E_f, v_m, E_m, ν_f, and ν_m are fiber-volume fraction, fiber elastic modulus, matrix-volume fraction, matrix elastic modulus, fiber Poisson's ratio, and matrix Poisson's ratio, respectively.

The transverse elastic modulus E_{22} and composite shear elastic modulus G_{12} were calculated by using

$$E_{22} = \frac{E_f E_m}{v_m E_f + v_f E_m} \tag{4}$$

$$G_{12} = \frac{G_f G_m}{v_m G_f + v_f G_m} \tag{5}$$

where G_f and G_m are fiber and matrix shear elastic moduli, respectively. (See refs. 9 and 10.) Table III lists the four graphite material properties obtained from using two different fiber-volume fractions (45 and 48 percent) in equations (2) to (5). The material properties at 50-percent fiber-volume fraction, which were developed in reference 1 and used in the tail boom design, are also included in table III.

DESCRIPTION OF FINITE ELEMENT MODEL

Geometry and Material Definition

The tail boom was modeled and analyzed by using the Engineering Analysis Language (EAL) finite element program (ref. 11). The finite element model for the tail boom skins consisted of two-dimensional, quadrilateral elements having combined membrane and bending stiffnesses. The tail boom skins have coupled extension and bending properties due to the unsymmetrical ply lay-up. The forward-attachment ring, stabilizer mounts, and end vertical fin supports were modeled with two-dimensional elements that had bending and extensional stiffnesses with no coupling. Beam elements were used for modeling forward-attachment fittings, ring frames, and aft bulkhead ring components.

The elastic mechanical properties of graphite/epoxy, E-glass/epoxy, and S-glass/epoxy used in modeling the tail boom are presented in tables III and IV. Table V gives the number of plies and total skin thicknesses used in the finite element model.

Since there were variations in skin thickness at the same station and from station to station, as shown in table I, the skin thicknesses were calculated in the following manner. The design skin thickness was used forward of station 49 since no test measurements were made there. The averages of the minimum and maximum measured skin thicknesses were used for all other stations except where large thicknesses were noted (stations 85.5, 169, and 172). The measurements taken at station 85.5 were questionable because of a 135-percent increase in thickness. The skin thickness measured at station 85.5 could have included the outer and inner portions of two ring frames located at stations 80 and 90.1. Therefore, the design skin thickness was

used for station 85.5. The averages of the minimum measured skin thickness and design skin thickness were used for the other two stations, 169 and 172.

Finite Element Models

Different finite element models were developed for the static and dynamic analyses. The static model, as shown in figure 6, had 401 nodes, 497 elements, and 2330 degrees of freedom. In order to simulate the static test conditions in reference 2, the static finite element model had all nodes at the forward end constrained in the three translational directions (X, Y, and Z). Since the static test had a load introduction structure at station 174, the finite element model included this structure. The dynamic finite element model was a derivative of the static model. The load introduction structure and the forward-end-constrained degrees of freedom used in the static finite element model were eliminated. The dynamic model, also shown in figure 6, had 376 nodes, 477 elements, and 2256 degrees of freedom. All nodes of the dynamic model had six degrees of freedom. Table VI gives the weight summary of the finite element model and the tail boom test model. In the dynamic finite element model, the test instrumentation was represented by point masses and the paint was assumed to be uniformly distributed on the tail boom skin.

RESULTS AND DISCUSSION

Comparison of Static Analysis With Test Results

Vertical and lateral static load tests were conducted on the tail boom and reported in reference 2. In the static tests, the tail boom was cantilevered at the forward end (station 32) and mounted to a backstop, as shown in figure 7. Displacements were measured at stations 110, 138, and 179. Figure 8 shows the locations of the displacement transducers used in the vertical and lateral static tests. Loads were applied from 20 to 300 lb in 20-lb increments and were introduced into the tail boom at station 179. Reference 2 contains a detailed description of the static test setup and instrumentation used. Finite element analyses of the vertical and lateral static load cases were conducted for three different graphite/epoxy skin fiber-volume fractions (45, 48, and 50 percent). Experimental and predicted results of the vertical displacements are presented in figure 9. The finite element results agree with the test results, with the best correlation being obtained for the 45-percent fiber-volume graphite/epoxy skin condition. Similar trends existed for the lateral load cases, as shown in figure 10. The difference between the test and finite element results for the 45-percent fiber volume ranged from 3 to 10 percent for the vertical and lateral load cases.

Comparison of Dynamic Analysis With Test Results

In the dynamic test, the tail boom was suspended with bungee cord to simulate a free-free boundary condition. Eleven accelerometer transducers were mounted on aluminum blocks at stations 32, 56, 79, 103, 126, 149, and 174, as shown in figure 11. Seven accelerometers were mounted vertically and four laterally. Reference 2 contains a detailed description of the test instrumentation and the type of modal analysis used in determining the natural frequencies. Four natural frequencies (first vertical and lateral bending and second vertical and lateral bending) were identified from the test. Dynamic finite element analyses were conducted for each of the three fiber-volume fraction conditions. Table VII lists the natural frequencies

identified from the test and analyses. The vertical and lateral frequencies were close for both the first and second bending modes, indicating that the vertical and lateral stiffnesses were about the same. The predicted natural frequencies and mode shapes for the first vertical and lateral modes of the 45-percent fiber volume agree with test results. The difference between test and predicted vertical and lateral natural frequencies ranged from 2 to 5 percent. The difference between test and predicted mode shapes varied from 15 to 48 percent for first vertical bending and from 19 to 24 percent for first lateral bending. Figures 12 and 13 show the experimental and predicted first vertical and lateral orthonormal mode shapes, respectively. These orthonormal mode shapes are modal vectors normalized to generalized mass and indicate that the calculated results have a structure that is stiffer than the test measurements.

CONCLUDING REMARKS

A static and dynamic finite element analysis of a U.S. Army OH-58 composite tail boom has been conducted and compared with test data. Because the actual tail boom skins were wet filament wound, there was a question as to which material properties to use in the model. Therefore, material tests were conducted on representative samples of the skins. Although the design fiber-volume fraction was 50 percent, the material tests revealed that the actual fiber-volume fraction varied from 44.6 to 49.3 percent. Static and dynamic finite element analyses were conducted for three fiber-volume fraction conditions of 45, 48, and 50 percent. The static and dynamic model with the 45-percent fiber-volume graphite skins gave the closest agreement with test data.

NASA Langley Research Center
Hampton, VA 23665-5225
August 22, 1985

REFERENCES

1. Taha, S.; Doerr, R.; and Messinger, R. H.: Environmental Effects and Durability Evaluation of Advanced Composite Fuselage Structure. USAAVRADCOM-TR-82-D-18, U.S. Army, Jan. 1983. (Available from DTIC as AD B070 815L.)

2. Calapoldas, Nick; and Hoff, Keith: Correlation of Results of an OH-58 Helicopter Composite Tail Boom Test With a Finite Element Model. AVSCOM TR 85-D-15, U.S. Army, 1985.

3. Rosato, D. V.; and Grove, C. S., Jr.: Filament Winding: Its Development, Manufacture, Applications, and Design. Interscience Pub., c.1964, pp. 145, 151.

4. Standard Test Methods for Specific Gravity and Density of Plastics by Displacement. ASTM Designation: D 792-66 (Reapproved 1979). Volume 08.01 of 1984 Annual Book of ASTM Standards, 1984, pp. 426-432.

5. Standard Test Method for Fiber Content of Resin-Matrix Composites by Matrix Digestion. ASTM Designation: D 3171-76 (Reapproved 1982). Volume 15.03 of 1984 Annual Book of ASTM Standards, 1984, pp. 169-172.

6. DOD/NASA Advanced Composites Design Guide. Volume IV - Materials, First ed. U.S. Air Force, July 1983, p. 3.

7. Dow, Norris F.; and Rosen, B. Walter: Evaluations of Filament-Reinforced Composites for Aerospace Structural Applications. NASA CR-207, 1965, pp. 9, 11.

8. Ashton, J. E.; Halpin, J. C.; and Petit, P. H.: Primer on Composite Materials: Analysis. Technomic Pub. Co., Inc., c.1969.

9. Jones, Robert M.: Mechanics of Composite Materials. Scripta Book Co., c.1975.

10. Dow, Norris F.; Rosen, B. Walter; and Hashin, Zvi: Studies of Mechanics of Filamentary Composites. NASA CR-492, [1966], pp. 27, 29.

11. Whetstone, W. D.: EISI-EAL Engineering Analysis Language Reference Manual - EISI-EAL System Level 2091. Engineering Information Systems, Inc., July 1983.

TABLE I.- GRAPHITE/EPOXY DESIGN AND MEASURED SKIN THICKNESSES

Station, in.	Measured skin thickness, in. (a)		Design skin thickness, in.
	Minimum	Maximum	
49	0.070	0.097	0.066
52	.063	.073	.068
65.5	.065	.071	.070
85.5	.153	.160	.075
107	.060	.065	.070
122	.060	.067	.061
137	.065	.067	.059
169	.085	.097	.069
172	.088	.099	.074

[a]Measurements include paint thickness (0.001 to 0.002 in.).

TABLE II.- GRAPHITE/EPOXY DENSITIES AND FIBER-VOLUME FRACTION AT STATION 49

Section	Composite density, lbm/in^3	Fiber-volume fraction, percent
6	0.0523	48.4
14	.0530	49.3
20	.0519	44.6

TABLE III.- MATERIAL PROPERTIES FOR GRAPHITE/EPOXY COMPOSITE USING EXPERIMENTAL DATA OBTAINED AT STATION 49

Fiber-volume fraction, percent	Longitudinal elastic modulus, E_{11}, psi	Transverse elastic modulus, E_{22}, psi	Composite shear elastic modulus, G_{12}, psi	Longitudinal Poisson's ratio, ν_{12}
45	15.5×10^6	0.809×10^6	0.470×10^6	0.294
48	16.5	.855	.493	.288
[a]50	17.2	.888	.509	.285

[a]Data obtained from reference 1.

TABLE IV.- MATERIAL PROPERTIES BASED ON 50-PERCENT FIBER VOLUME OBTAINED FROM REFERENCE 1

Material	Longitudinal elastic modulus, E_{11}, psi	Transverse elastic modulus, E_{22}, psi	Composite shear elastic modulus, G_{12}, psi	Longitudinal Poisson's ratio, ν_{12}	Composite density, lbm/in^3
E-glass	6.0×10^6	1.4×10^6	0.60×10^6	0.25	0.060
S-glass	7.1	1.4	.55	.25	.056

TABLE V.- SKIN THICKNESSES OF FINITE ELEMENT MODEL

Station, in.	Number of plies	Total skin thickness, in.
32	8	0.064
42.8	8	.066
56.2	7	.068
67.6	7	.068
79	7	.070
84.6	7	.075
90.2	7	.078
102.8	5	.063
114.4	5	.063
126	5	.063
137.7	5	.066
149.3	5	.066
161.2	5	.070
173.1	5	.074
179.8	5	.085

TABLE VI.- TAIL BOOM WEIGHT SUMMARY

Description	Calculated weight, lb (a)	Measured weight, lb (b)
Tail boom shell and ring frames	23.27	
Forward-attachment assembly unit	3.40	
Exterior support structures	2.27	
Paint	3.00	
Total	31.94	31.94

[a]Calculated weight for finite element model.
[b]Measured weight obtained from reference 2.

TABLE VII.- TEST AND ANALYTICAL NATURAL FREQUENCIES

Natural bending mode	Test natural frequency, Hz	Analytical natural frequency, Hz, for fiber volume of -		
		45 percent	48 percent	50 percent
First vertical	75.37	79.47	81.94	83.54
First lateral	77.34	79.27	81.72	83.30
Second vertical	226.05	221.17	227.80	232.06
Second lateral	222.16	215.80	222.30	226.45

Figure 1.- U.S. Army OH-58 observation helicopter. L-85-126

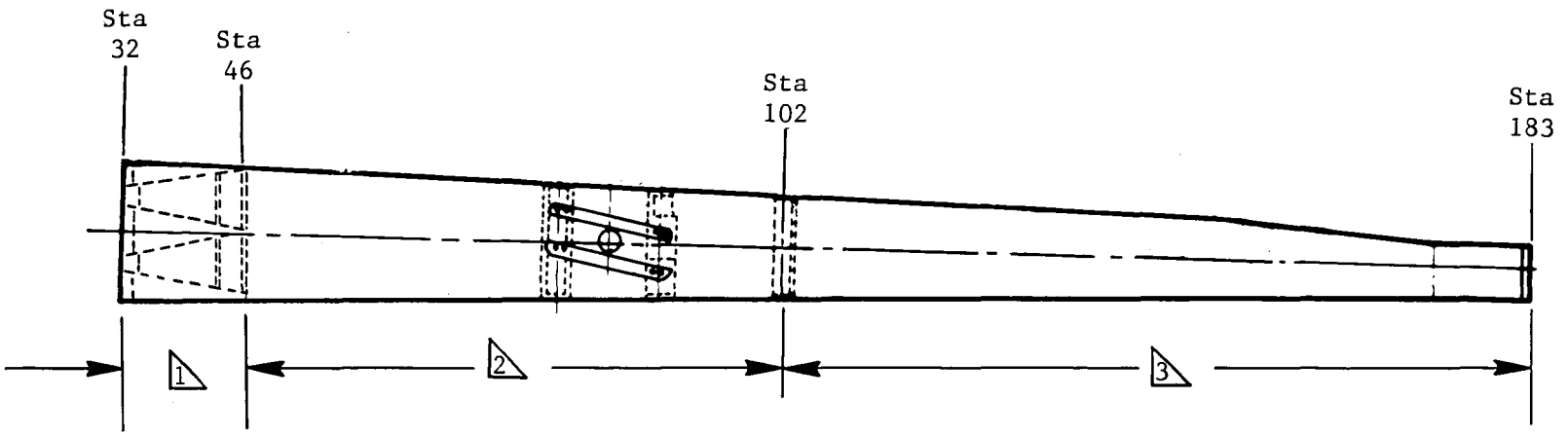

Skin ply sequence

1	$[90^{\circ}/\pm 60^{\circ}/\pm 25^{\circ}_{2}/90^{\circ}]$	8 plies
2	$[\pm 60^{\circ}/\pm 25^{\circ}_{2}/90^{\circ}]$	7 plies
3	$[\pm 25^{\circ}_{2}/90^{\circ}]$	5 plies

Figure 2.- Tail boom stations and ply sequence. All dimensions are given in inches unless otherwise specified.

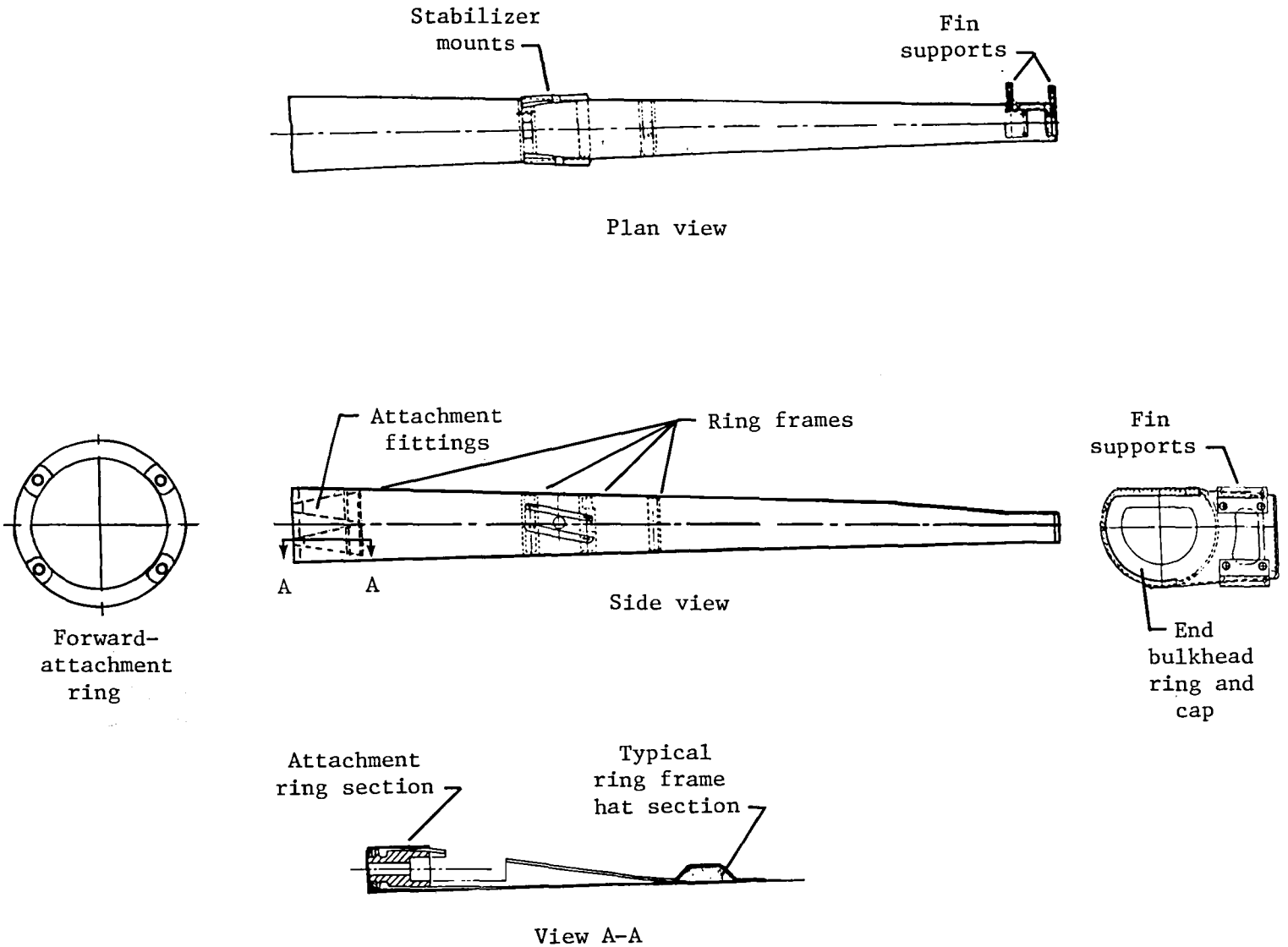

Figure 3.- Tail boom components.

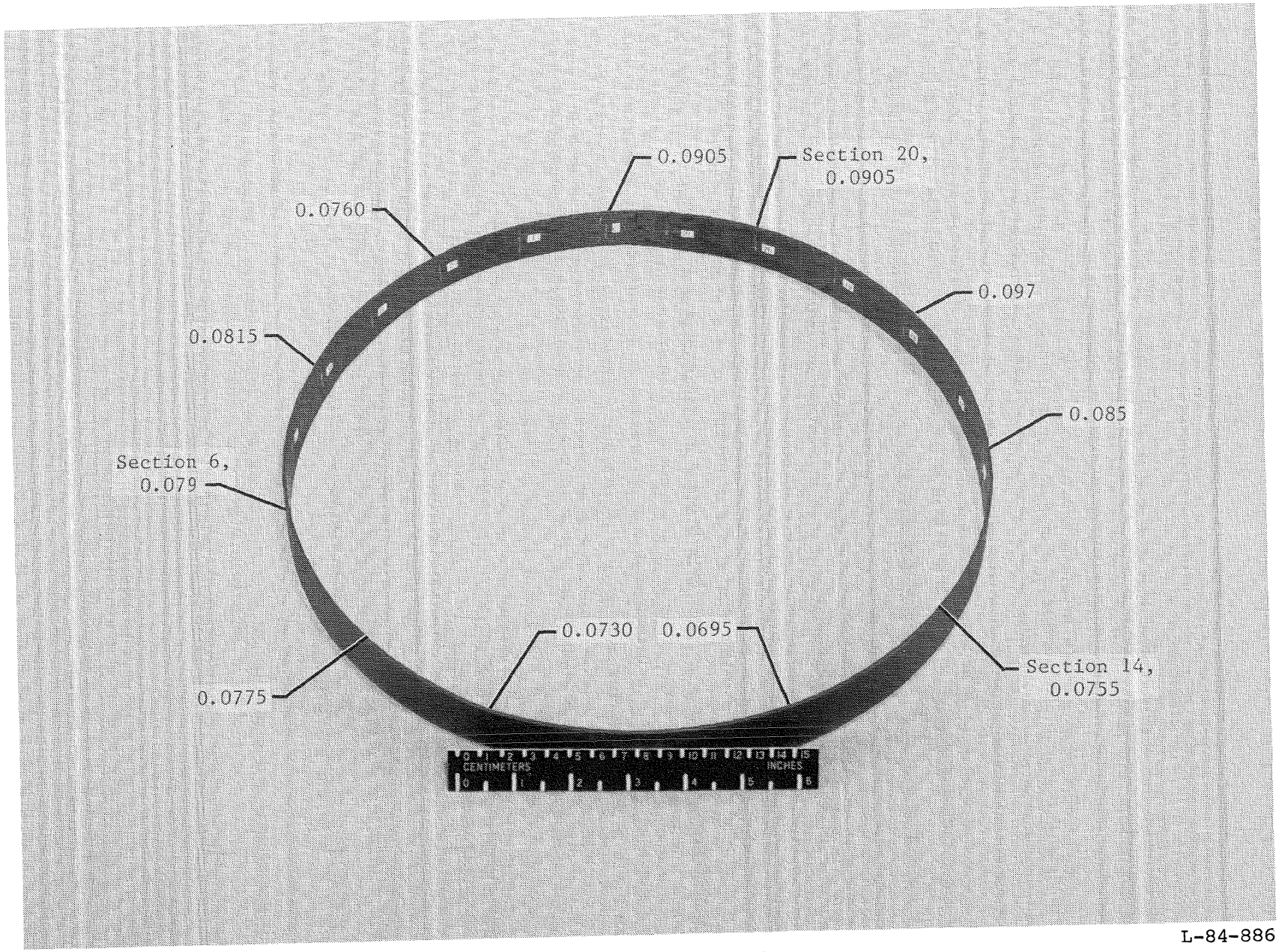

L-84-886

Figure 4.- Skin thicknesses at station 49. All dimensions are given in inches.

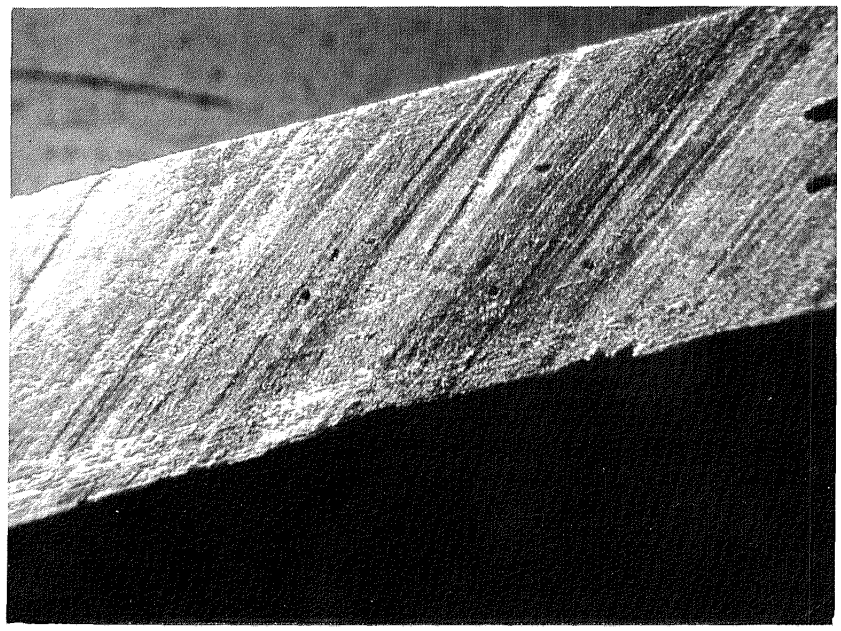

(a) 1.5-percent voids by volume.

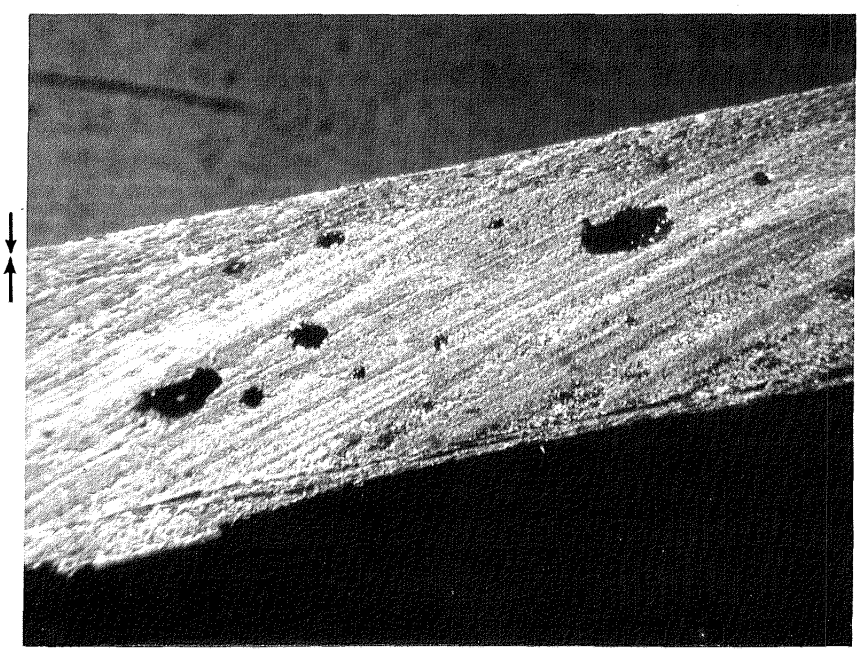

(b) 5-percent voids by volume.

L-85-127

Figure 5.- Photomicrographs of two locations on station 49. Magnification ×20.

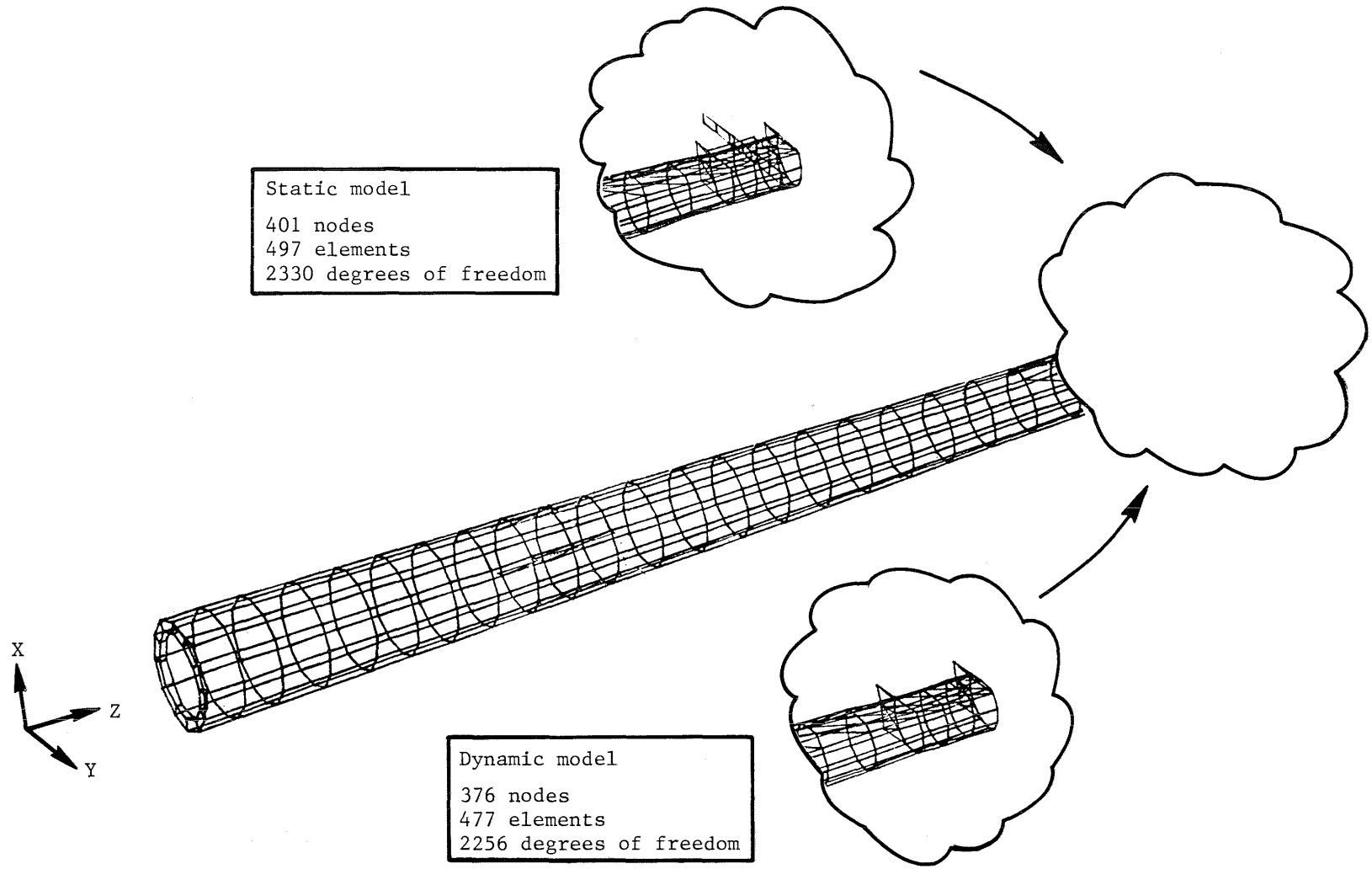

Figure 6.- EAL finite element models.

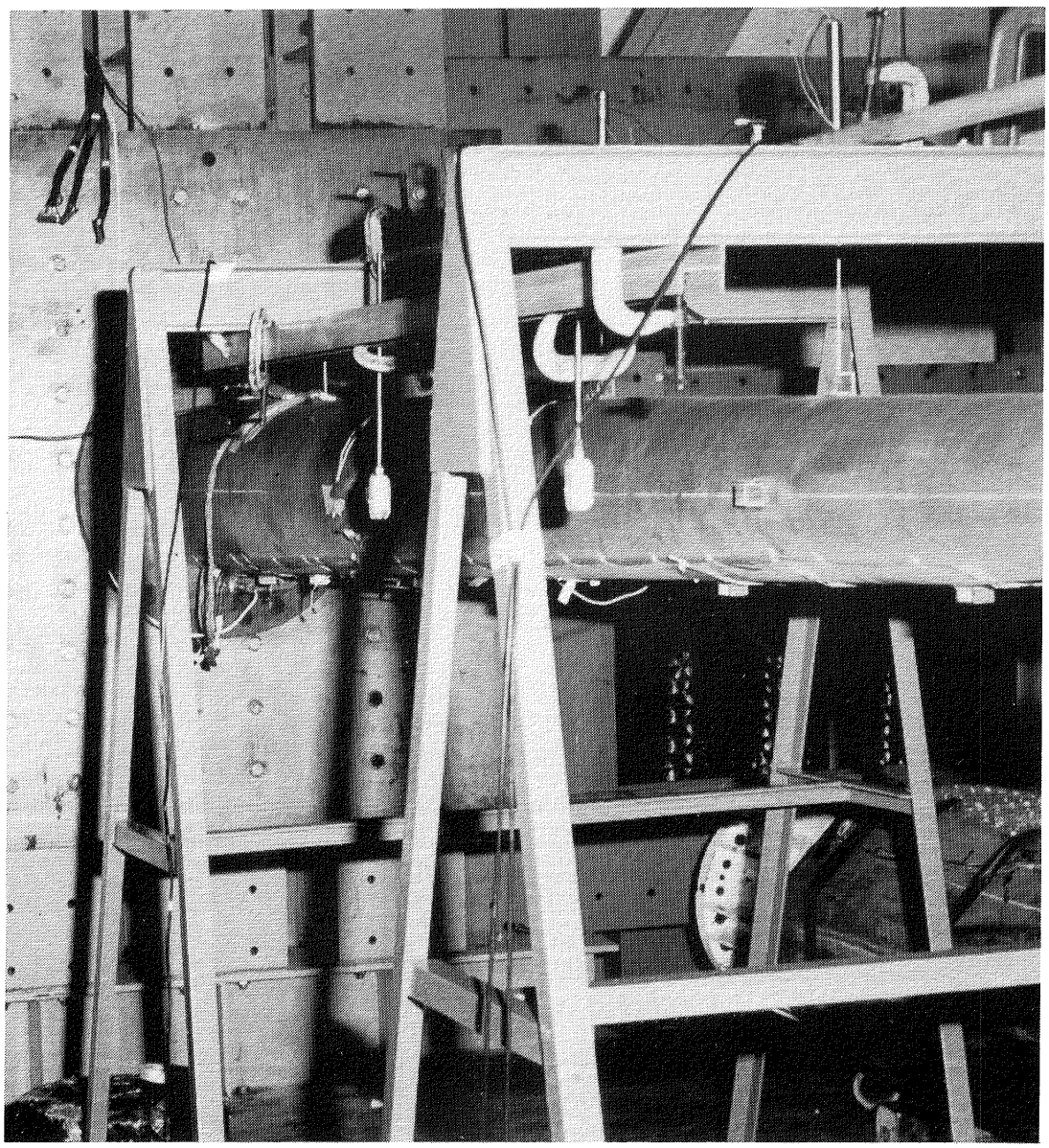

L-85-128

Figure 7.- Static test setup.

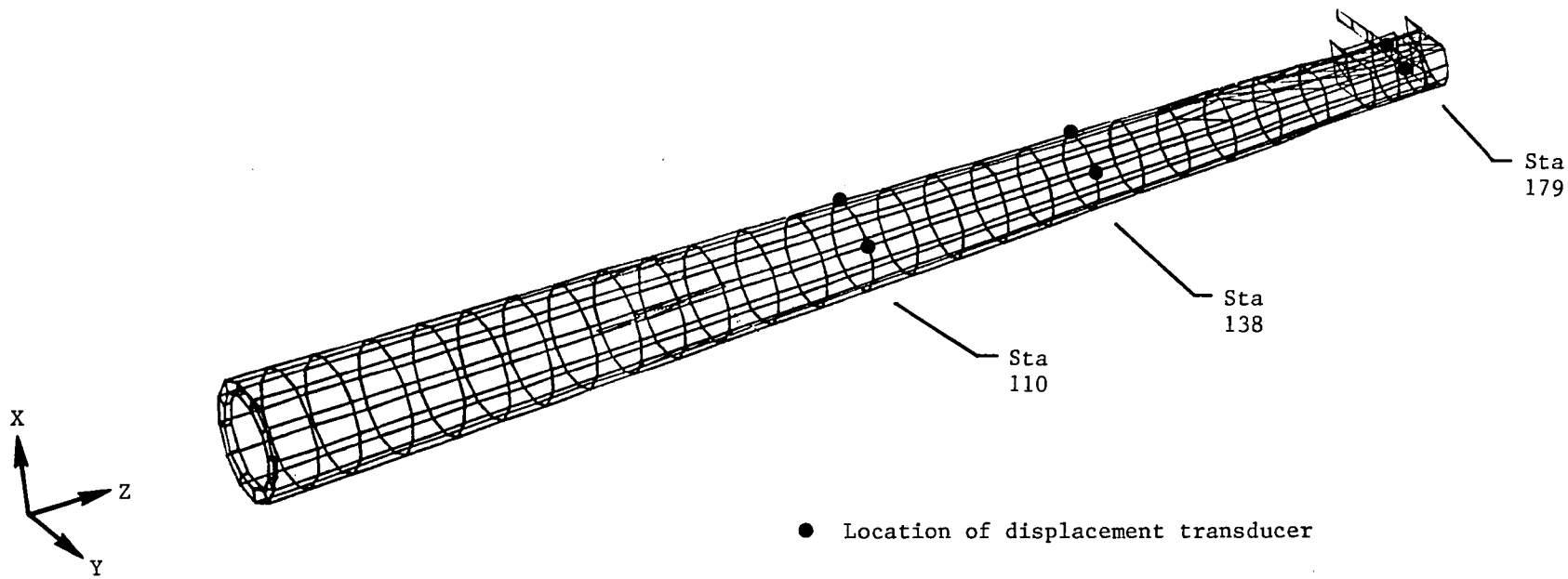

Figure 8.- Locations of displacement transducers used in vertical and lateral static tests.

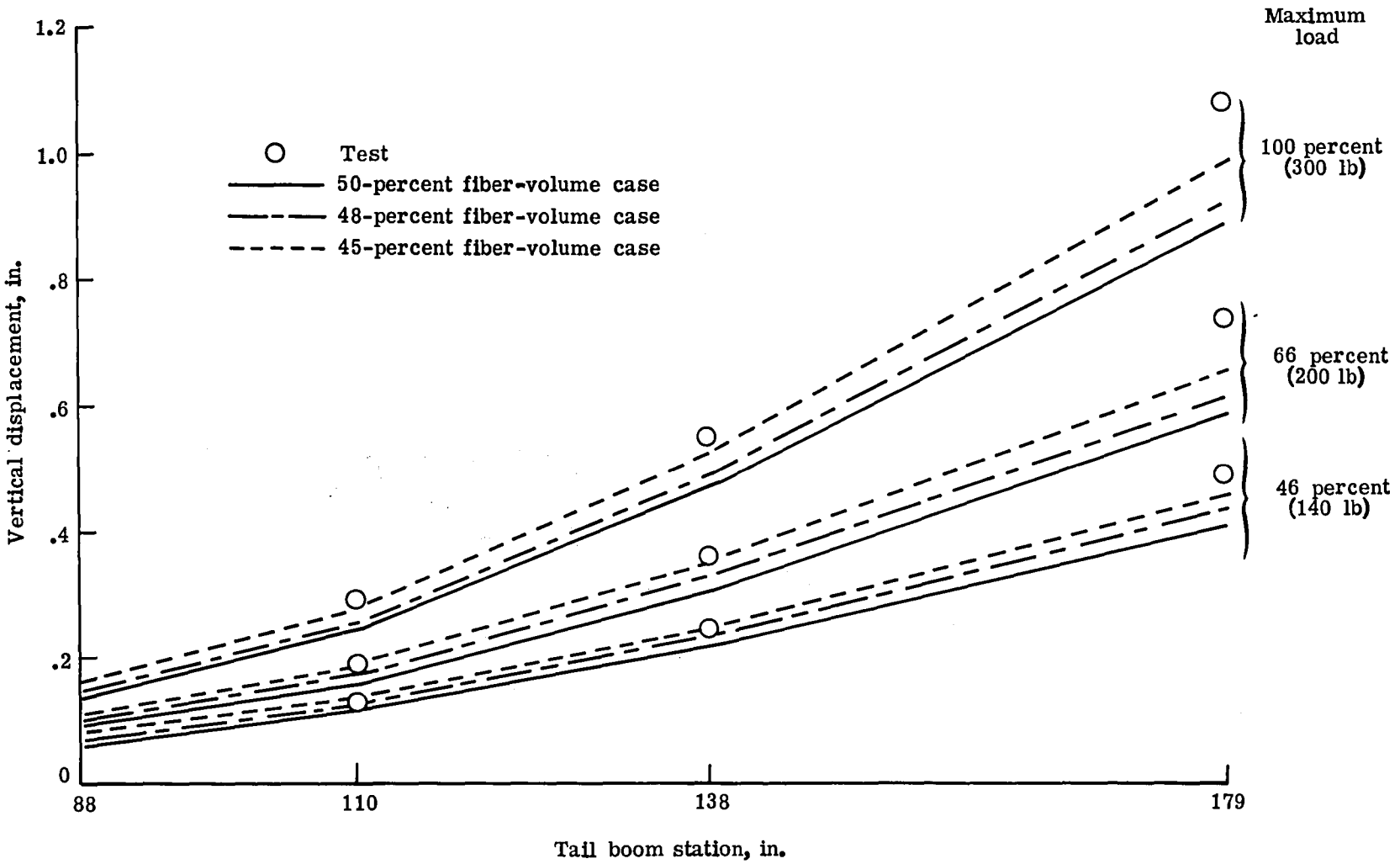

Figure 9.- Vertical displacement plotted against tail boom station.

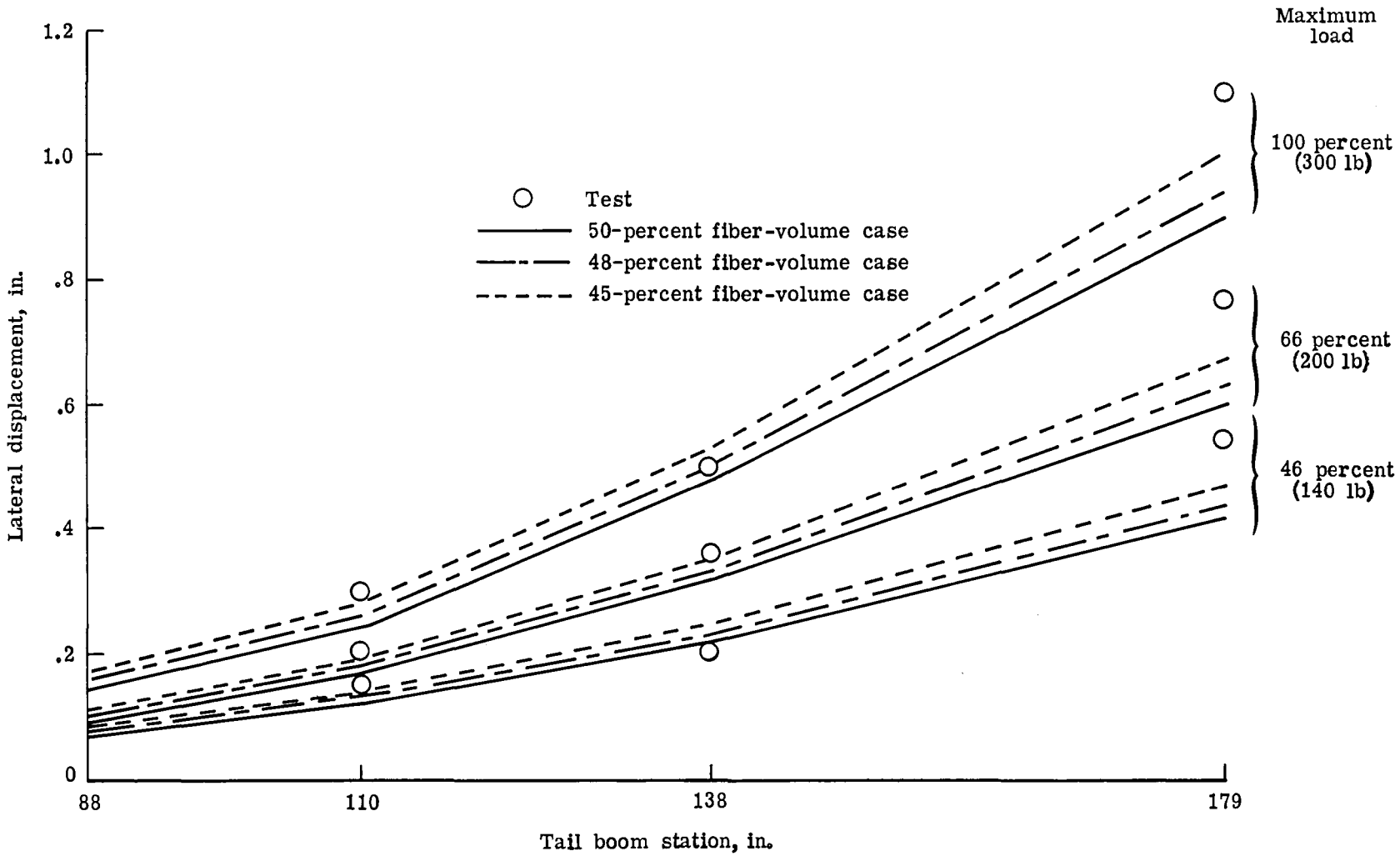

Figure 10.- Lateral displacement plotted against tail boom station.

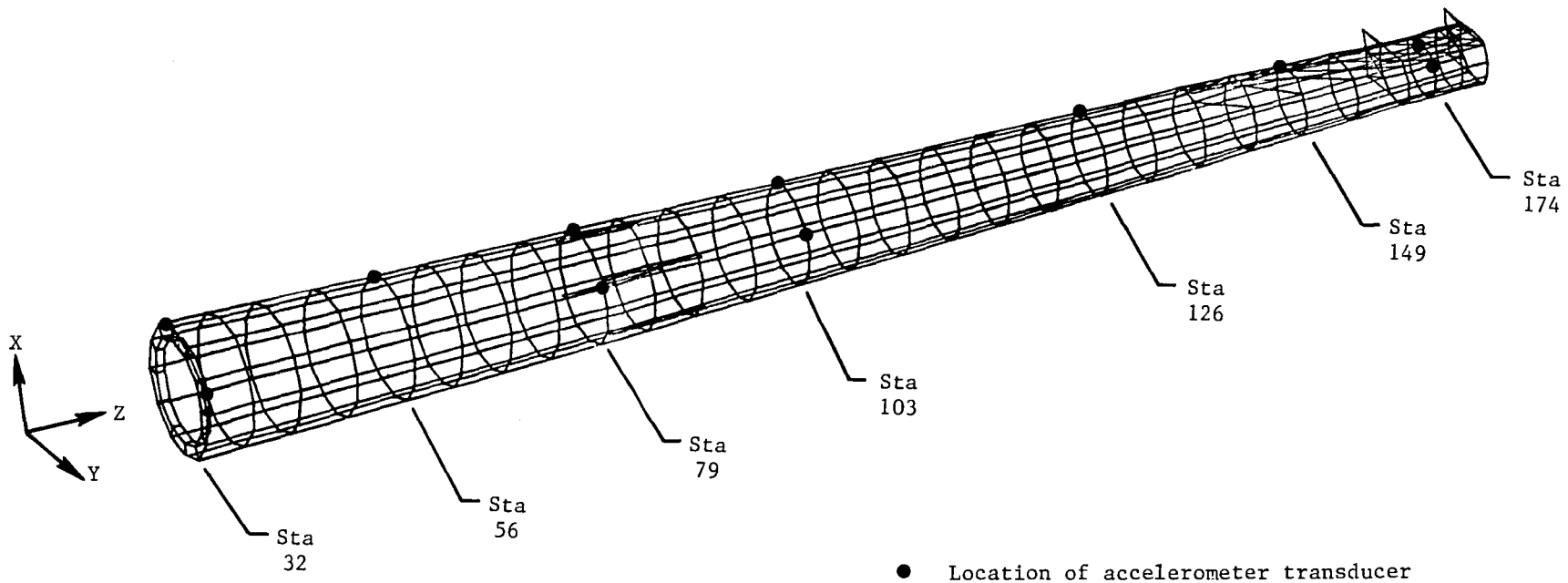

Figure 11.- Locations of accelerometer transducers used in vertical and lateral dynamic tests.

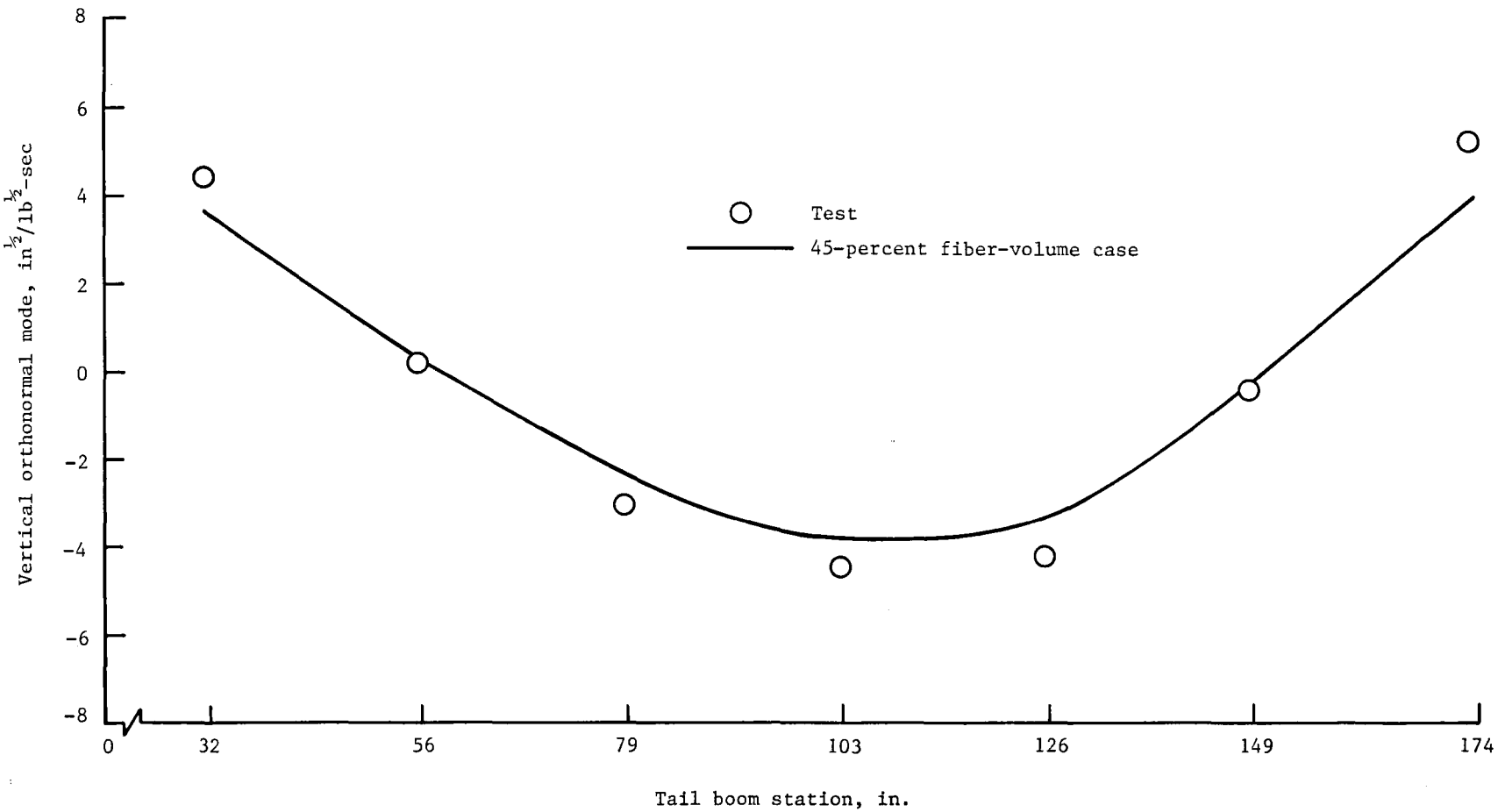

Figure 12.- First vertical orthonormal bending mode.

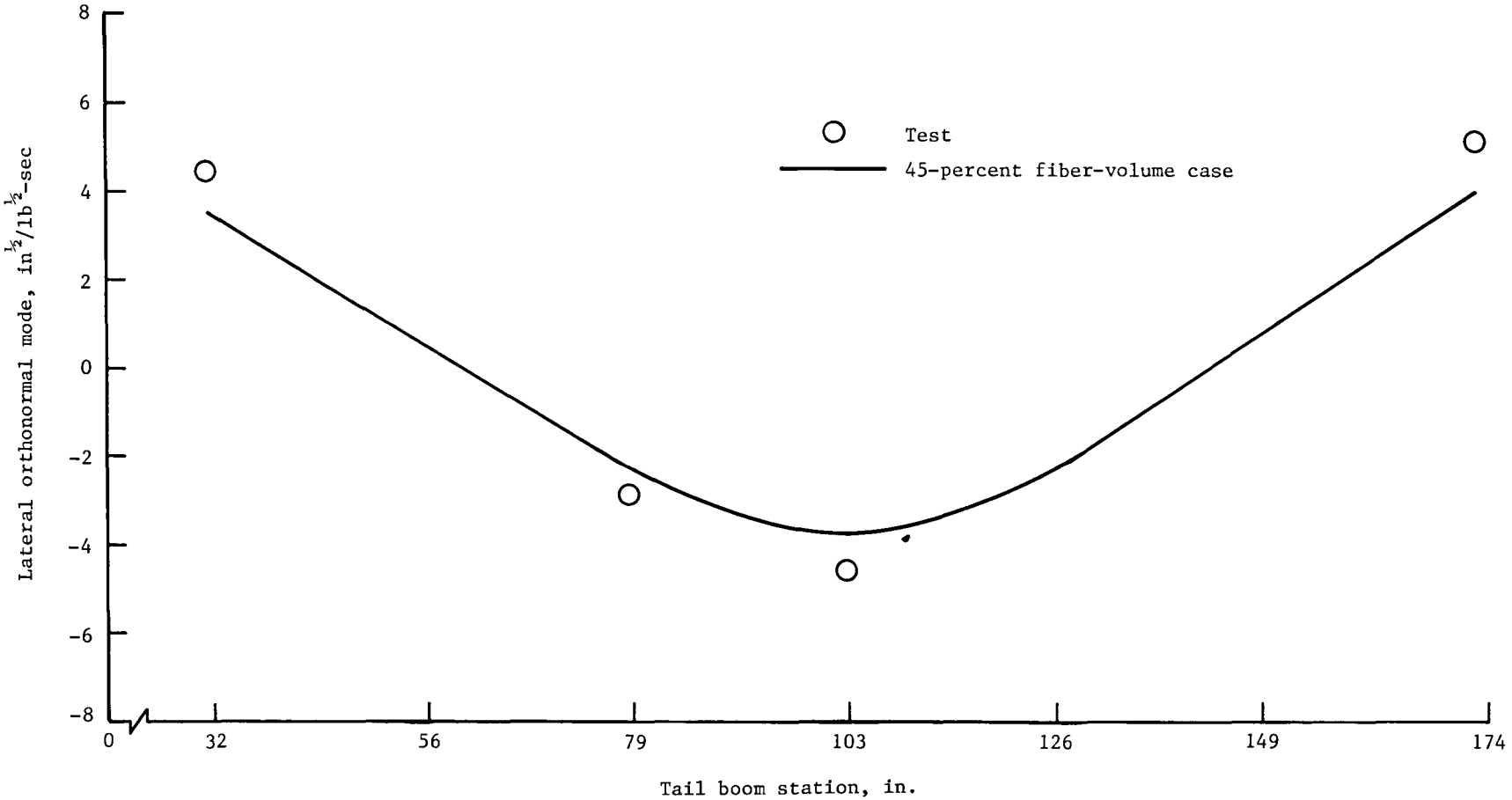

Figure 13.- First lateral orthonormal bending mode.

1. Report No.	2. Government Accession No.	3. Recipient's Catalog No.
NASA TM-86430 AVSCOM TR 85-B-5		

4. Title and Subtitle	5. Report Date
Effect of Measured Material Properties on the Finite Element Analysis of an OH-58 Composite Tail Boom	October 1985
	6. Performing Organization Code 505-42-39-02

7. Author(s)	8. Performing Organization Report No.
Lynn M. Bowman	L-15969
	10. Work Unit No.

9. Performing Organization Name and Address	11. Contract or Grant No.
Aerostructures Directorate USAARTA-AVSCOM NASA Langley Research Center Hampton, VA 23665-5225	

12. Sponsoring Agency Name and Address	13. Type of Report and Period Covered
National Aeronautics and Space Administration Washington, DC 20546-0001 and U.S. Army Aviation Systems Command St. Louis, MO 63120-1798	Technical Memorandum
	14. Army Project No. 1L161102AH45

15. Supplementary Notes

Lynn M. Bowman: Aerostructures Directorate, USAARTA-AVSCOM, Langley Research Center, Hampton, Virginia.

16. Abstract

A static and dynamic finite element analysis was conducted on a U.S. Army OH-58 composite tail boom and compared with test data. The tail boom was a filament-wound graphite/epoxy monocoque structure. The structural design of the composite tail boom skin was based on 50-percent graphite fiber volume. However, material tests on representative samples of the tail boom skin revealed that the graphite fiber-volume fraction varied from 44.6 to 49.3 percent. To determine the effect of using measured material properties, static and dynamic finite element analyses were conducted for three fiber-volume conditions of 45, 48, and 50 percent. The static and dynamic model with the 45-percent fiber-volume graphite skins gave the closest agreement with test data.

17. Key Words (Suggested by Author(s))	18. Distribution Statement
Tail boom OH-58 helicopter Composite structure Filament winding Finite element analysis	Unclassified - Unlimited Subject Category 24

19. Security Classif. (of this report)	20. Security Classif. (of this page)	21. No. of Pages	22. Price*
Unclassified	Unclassified	25	A02

*For sale by the National Technical Information Service, Springfield, Virginia 22161

End of Document